Removing Diurnal Cycle Contamination in Satellite-Derived Tropospheric Temperatures: Understanding Tropical Tropospheric Trend Discrepancies

Stephen Po-Chedley, Tyler J. Thorsen, and Qiang Fu

Department of Atmospheric Sciences, University of Washington, Seattle, Washington

ABSTRACT

Independent research teams have constructed long-term tropical time series of the temperature of the middle troposphere (TMT) using satellite Microwave Sounding Unit (MSU) and Advanced MSU (AMSU) measurements. Despite careful efforts to homogenize the MSU/AMSU measurements, tropical TMT trends beginning in 1979 disagree by more than a factor of 3. Previous studies suggest that the discrepancy in tropical TMT trends is caused by differences in both the *NOAA-9* warm target factor and diurnal drift corrections. This work introduces a new observationally based method for removing biases related to satellite diurnal drift. Over land, the derived diurnal correction is similar to a general circulation model (GCM) diurnal cycle. Over ocean, the diurnal corrections have a negligible effect on TMT trends, indicating that oceanic biases are small. It is demonstrated that this method is effective at removing biases between coorbiting satellites and biases between nodes of individual satellites. Using a homogenized TMT dataset, the ratio of tropical tropospheric temperature trends relative to surface temperature trends is in accord with the ratio from GCMs. It is shown that bias corrections for diurnal drift based on a GCM produce tropical trends very similar to those from the observationally based correction, with a trend difference smaller than $0.02 \, \mathrm{K \, decade^{-1}}$. Differences between various TMT datasets are explored further. Large differences in tropical TMT trends between this work and that of the University of Alabama in Huntsville (UAH) are attributed to differences in the treatment of the *NOAA-9* target factor and the diurnal cycle correction.

1. Introduction

Atmospheric deep layer temperature trends from satellite Microwave Sounding Unit (MSU) and Advanced MSU (AMSU) measurements are frequently used both as a measure of climate change and as a reference to evaluate general circulation models (GCMs) (e.g., Wallace et al. 2000; Santer et al. 2005; Karl et al. 2006; Solomon et al. 2007; Fu et al. 2011; Po-Chedley and Fu 2012b). A common metric is to compare the ratio of warming between the troposphere and the surface in the tropics since GCMs and basic atmospheric physics suggest that tropospheric temperature change should be amplified relative to surface temperature change.

Over the past decade many studies based on MSU/AMSU observations have shown that the tropical tropospheric temperature increases more than the surface

temperature on multidecadal time scales (Fu et al. 2004; Fu and Johanson 2005; Mears and Wentz 2005, Thorne et al. 2007; Santer et al. 2008), while others suggest reduced tropospheric warming relative to the surface (e.g., Christy et al. 2007, 2010; Douglass et al. 2008). Our understanding of tropical tropospheric temperature trends is complicated by the fact that tropical radiosonde stations are limited in number, their trends are cold biased, and the bias magnitude cannot be accurately determined (e.g., Sherwood et al. 2005; Randel and Wu 2006; Titchner et al. 2009). Complications with radiosonde measurements reinforce the need to ensure that satellite records are unbiased in order to advance our understanding of climate and climate change.

Three research teams, including the University of Alabama in Huntsville (UAH), Remote Sensing Systems (RSS), and the National Oceanic and Atmospheric Administration (NOAA) Center for Satellite Applications and Research (STAR), have developed up-to-date, homogenized datasets for the temperature of the middle troposphere (TMT) (Christy et al. 2003; Mears et al. 2003; Zou and Wang 2011). These groups employ over 30 years

Corresponding author address: Stephen Po-Chedley, Department of Atmospheric Sciences, Box 351640, University of Washington, Seattle, WA 98195.
E-mail: pochedls@uw.edu

of temperature measurements from MSU and, starting in 1998, AMSU. These instruments have flown on board a number of satellites, beginning with MSU on TIROS-N in late 1978 through AMSU on *NOAA-19*. Despite using the same basic radiometer measurements, tropical TMT trend differences between these groups differ by more than a factor of 3. The UAH dataset has a tropical TMT trend that is close to zero ($0.029\,\text{K decade}^{-1}$), whereas RSS and NOAA have trend values of 0.089 and $0.105\,\text{K decade}^{-1}$, respectively. Zou et al. (2009) analyzed TMT trends over the tropical ocean, where the diurnal drift effects are negligible for trend comparisons. They found large trend differences between MSU/AMSU datasets and enhanced tropical tropospheric amplification relative to both RSS and UAH. Reasons for TMT trend differences stem from different processing choices and bias corrections made by the three research teams, including the choice of satellites included (Mears et al. 2003), corrections for the influence of the warm target temperature on the measured brightness temperature (e.g., Christy et al. 2000; Mears et al. 2003; Po-Chedley and Fu 2012a), and corrections for the drift of satellites through the diurnal cycle (e.g., Christy et al. 2000; Fu and Johanson 2005; Mears and Wentz 2005). Recent studies by Po-Chedley and Fu (2012a, 2013) suggest that UAH uses a biased *NOAA-9* warm target factor that results in artificial cooling in the UAH TMT time series, though UAH has not changed its treatment of *NOAA-9* (Christy and Spencer 2013). Accounting for this bias, however, can only explain part of the discrepancy in TMT trends between UAH and other teams over the tropics. Much of the remaining discrepancies in TMT trends are likely caused by differences in diurnal drift corrections employed by various MSU/AMSU research teams.

As a polar-orbiting satellite drifts east or west relative to the sun, the local sampling time on Earth, generally indicated by the local equatorial crossing time (LECT), changes accordingly (Fig. 1). As the satellite drifts over time, changes in the satellite-measured brightness temperature due to changes in the local sampling time can be much larger than the temperature change associated with the long-term climate change. This is especially true over land where the surface skin temperature has a large diurnal range. It is therefore very important to remove the effect of diurnal drift on the measured brightness temperature when estimating the magnitude of decadal temperature change. The RSS and NOAA research teams apply a drift correction based on the diurnal cycle from a GCM (Mears et al. 2003; Zou and Wang 2011), whereas UAH produces an MSU TMT diurnal correction based on temperature comparisons between three coorbiting satellites carrying AMSU with different local sampling times. UAH does not yet correct
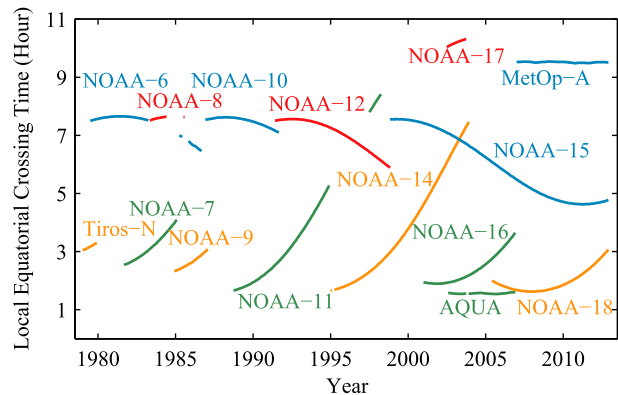

FIG. 1. LECT for the satellites used in this study. We include LECT values for all the months in which satellites are incorporated into our analysis. LECTs in this figure are for the descending node. LECTs for the ascending node are 12 h later.

the diurnal drift for satellites carrying AMSU, because they attempt to use these satellites during periods when diurnal drift is small (J. Christy 2013, personal communication). By comparing MSU/AMSU datasets with radiosondes, several studies suggest that diurnal adjustments derived from a GCM and/or other bias corrections lead to a warm bias in the trends for lower-tropospheric temperature data (TLT) for RSS (Christy and Norris 2006; Christy et al. 2007; Randall and Herman 2008; Christy et al. 2010). Mears et al. (2012) found that many of the conclusions from these studies were dependent on the datasets and time considered and found that the methodological choices significantly impacted the results. Mears et al. (2012) also point out that the time period considered is complicated by effects from ENSO and the eruption of Mount Pinatubo. In addition, radiosonde networks undergo artificial cooling, which may not be completely removed (Sherwood et al. 2005, 2008). In general, it is impossible to conclude which dataset is most accurate when comparing two potentially biased measurements (Mears et al. 2012).

This paper focuses on developing a novel approach to the diurnal drift correction based on MSU/AMSU observations. We use MSU/AMSU level 1 data calibrated with an instrument calibration technique that minimizes intersatellite differences, reducing intersatellite residuals by an order of magnitude compared to the prelaunch MSU/AMSU calibration (Zou et al. 2009). This state-of-the-art instrument calibration allows us to derive a diurnal drift correction by attributing remaining intersatellite differences to diurnal drift biases. In section 2, we describe the data that we use in this study and list comparison datasets. We describe our basic processing decisions for homogenizing MSU/AMSU level 1 data in section 3. In section 4, we present an observationally based approach for removing biases related to the diurnal drift of

satellites and compare this correction to the GCM-derived correction. We then show the efficacy of our approach with an emphasis on the tropics. Our homogenized TMT time series is compared to the UAH, RSS, and NOAA TMT products in section 5, and, in section 6, we attempt to understand major underlying causes for differences. In section 7, we conclude with a summary and discussion of our results.

2. Data

a. Level 1 MSU/AMSU dataset

In this study, we use the most recent version of the level 1C (L1C) MSU/AMSU data produced by NOAA STAR, which was newly released in 2013. The dataset has been described by Zou and Wang (2011, 2013). The L1C data have been intercalibrated using simultaneous nadir overpasses (SNO) (Zou et al. 2006; Zou and Wang 2011). This on-orbit calibration technique utilizes simultaneous nadir observations in polar regions from coorbiting satellites to solve for the MSU/AMSU calibration coefficients such that intersatellite biases related to the warm target temperature are minimized. The L1C swath data minimize or remove a number of biases using the NOAA STAR Integrated Microwave Intercalibration Approach (IMICA).

The NOAA IMICA calibration is both effective and important to our analysis. The limb view correction used in IMICA removes temperature differences due to vertical sampling differences across view angles with accuracy below the noise of the instrument, and the corrected temperatures have similar distributions for the limb and near-nadir measurements (Goldberg et al. 2001). Zou et al. (2009) found that the trends are independent of the number of footprints used, implying that the limb correction does not have a large influence on our results, and our product effectively represents the nadir view of the MSU/AMSU instrument. *NOAA-16* exhibits steady bias drifts in the radiometer signal counts, which leads to a spurious warm drift of ~0.3 K decade^{-1} in the brightness temperatures (Zou and Wang 2011). For this reason, RSS does not include *NOAA-16* in its analysis. This bias drift is removed in the IMICA analysis, which allows us to consider *NOAA-16* data in our analysis, though the inclusion of these data does not significantly affect the diurnal cycle correction derived in this work. The IMICA calibration also minimizes biases related to sun heating instrument variability and the scene temperature, which may introduce regional and seasonal biases and spurious trends (Zou and Wang 2011). Using IMICA, the global ocean mean intersatellite bias and standard deviation is on the order of 0.05 and 0.03 K, respectively, compared to the prelaunch calibration, which has biases on the order of 0.5 and 0.13 K (Zou and

Wang 2013). IMICA brings intersatellite trends close to zero over the ocean (Zou et al. 2009). Since the diurnal drift effect is small over the ocean, this implies that the instrument calibration is excellent.

In summary, the IMICA procedure removes biases, including (i) global mean intersatellite biases, (ii) scene-temperature-dependent biases due to inaccurate calibration nonlinearity, (iii) sun-heating-induced instrument variability biases, (iv) drift bias for *NOAA-16*, and (v) limb adjustment to nadir (Zou and Wang 2011; C.-Z. Zou 2013, personal communication). Because the IMICA calibration eliminates or minimizes these biases, we are able to largely attribute remaining intersatellite differences to diurnal drift effects, though we cannot completely rule out unknown biases. Note that any unknown residual biases that are correlated with the diurnal cycle but independent of individual satellite ascending and descending nodes will effectively be removed through our diurnal cycle correction.

b. Comparison datasets

To compare our MSU/AMSU TMT homogenization and merging efforts to independent datasets, we utilize the most recent versions of existing MSU/AMSU climate records, including UAH TMT v5.6 (Christy et al. 1998, 2000, 2003), RSS TMT v3.3 (Mears et al. 2003; Mears and Wentz 2009; Mears et al. 2011), and NOAA TMT v3.0 (Zou et al. 2006, 2009; Zou and Wang 2010, 2011). We also employ temperatures from lower-stratospheric channel data (TLS) from these groups in order to remove the stratospheric signal from the TMT dataset (e.g., Fu et al. 2004). These datasets represent independently homogenized monthly MSU/AMSU datasets that can be used for comparison to our work. We also utilize HadCRUT4 data as a measure of surface temperature trends over land and ocean (Morice et al. 2012).

The largest differences between MSU/AMSU datasets relate to how each group removes instrument calibration drift and biases due to diurnal drift. UAH applies a diurnal drift correction for MSU based on the diurnal cycle derived from coorbiting AMSU measurements and avoids using data when large diurnal drifts are present. RSS and NOAA utilize corrections based on the diurnal cycle simulated by a climate model. RSS and UAH generally utilize the prelaunch calibration, whereas NOAA (and this analysis) utilizes data that are corrected using IMICA. All of the datasets remove residuals related to the warm target temperature on board the satellite, though differences in methodology lead to different bias corrections (e.g., Po-Chedley and Fu 2013). Another difference relates to how data are included in the merging procedure. RSS and NOAA use a consensus approach that averages all overlapping satellites together. UAH

chooses stable backbone reference satellites and ignores data when diurnal drifts noticeably affect the time series (e.g., Christy and Spencer 2013). Other differences include corrections to limb data, removing differences between MSU and AMSU measurements, and how scene-dependent temperature biases are removed.

3. Procedures and processing decisions for L1C MSU/AMSU data

We begin our analysis with NOAA STAR L1C data, utilizing MSU channel 2 and AMSU channel 5 data over 1979–2012. These two channels have historically been used to represent the midtropospheric temperature. We use the 5 central view angles from MSU and 12 central view angles for AMSU (e.g., Mears and Wentz 2009). We correct the L1C data for diurnal drift by adjusting the data to local noon utilizing a GCM-derived diurnal cycle, while we also process L1C data with no diurnal correction, which we will use to derive and apply an observationally based diurnal correction developed in this study (see section 4). For quality control purposes, we remove measurements that are greater than 5σ above or below the daily zonal (2.5°) average brightness temperature for each satellite. Daily data are then placed into $2.5° \times 2.5°$ grids for the ascending and descending nodes. Measurements that are more than 4σ above or below the long-term grid point mean are eliminated. Both of these quality control steps remove less than 0.07% of the data for each satellite. Following Wang and Zou (2014), we remove observations that contain precipitation. We also manually removed data in cases when the data are suspect, including TIROS-N after 1979, *NOAA-6* after day 274 of 1986, *NOAA-9* after day 62 of 1987, *NOAA-14* after 2003, *NOAA-16* and *Aqua* beginning in 2007, and *NOAA-17* after day 300 of 2003. Several individual days were also removed as a result of obvious data quality issues.

After quality control and gridding, we follow Mears et al. (2003) to remove the warm target temperature effect. The warm target temperature effect was described by Christy et al. (2000), in which it was determined that the evolution of the warm target calibration temperature on board various satellites could explain intersatellite differences between coorbiting satellites. This issue is caused by sun-heating-induced instrument variability and is largely removed via the IMICA calibration (Zou and Wang 2011), but we apply the warm target temperature calibration to remove any remaining residuals. Following Mears et al. (2003), we used global mean oceanic pentad (5-day averages) data to linearly regress out any intersatellite difference residuals related to the warm target temperature on board each satellite. The regression uses

intersatellite brightness temperature differences as predictands and warm target temperature anomalies on board each satellite as predictors. The coefficients of this regression are referred to as warm target factors. In constructing global mean pentads, we required that each pentad had data from 85% of the ocean grid cells and that there were at least three days of data. By using oceanic data to determine the warm target factors, the influence of the diurnal cycle is minimized, since the diurnal cycle over the ocean is approximately an order of magnitude smaller than over land. We solved for our target factors using oceanic data that were diurnally corrected with the RSS climate model data, but the differences in our target factors and the resulting temperature trends are negligible if we use oceanic data that have no diurnal correction.

After solving for the target factors, we create monthly averages for each satellite's ascending and descending nodes and utilize our target factors to remove the warm target temperature effect from each grid cell. To remove MSU/AMSU differences related to differences in the weighting function we take the monthly average value for *NOAA-15* minus *NOAA-14* over 1999 through 2003 to create an average monthly offset climatology for each satellite node following Mears and Wentz (2009). In computing our monthly gridded data, this offset climatology is removed from the AMSU data to match AMSU with MSU, as in Mears and Wentz (2009).

4. Diurnal drift corrections

a. GCM-based diurnal drift correction

To remove diurnal drift from TMT measurements, the RSS team uses the diurnal cycle simulated from five years of model simulation in the National Center for Atmospheric Research Community Climate System Model, version 3 (CCSM3), (Kiehl et al. 1996; Mears et al. 2003). Mears et al. (2003) derived the TMT diurnal cycle with hourly data for each month of the year and each view angle using microwave radiative transfer and surface emissivity models (Wentz and Meissner 1999). We use the RSS diurnal correction and scale the diurnal amplitude by 0.875 for MSU and 0.917 for AMSU following Zou and Wang (2009).

The diurnal drift correction is sensitive to the applied diurnal cycle in terms of both phase and amplitude (Po-Chedley 2012). Dai and Trenberth (2004) showed that the GCM-simulated diurnal cycle in CCSM2 likely has biases. Therefore, model biases may impact diurnal bias corrections applied from GCM data. It has been suggested that RSS and NOAA overcorrect for diurnal drift, which leads to spurious warming relative to UAH in the tropics (Christy et al. 2010, 2011). On the other hand, NOAA (Zou and Wang 2009) and RSS

(Mears et al. 2003) have compared the magnitude of the GCM-derived diurnal drift correction with global intersatellite residuals and have shown that the adjustments applied minimize intersatellite residuals. Other studies have also found consistency between GCM-derived and observed diurnal cycle climatology in tropospheric channels of the High-Resolution Infrared Radiation Sounder, which provides evidence that diurnal cycle climatology from a GCM should be reasonably valid for microwave measurements (Jackson and Soden 2007; MacKenzie et al. 2012).

Because it is possible that GCM-derived diurnal cycle corrections have biases, we develop a regression technique to derive a TMT diurnal cycle correction based on satellite observations for the purpose of homogenizing the MSU/AMSU observations. This diurnal correction will be used as a comparison to understand the corrections implemented by NOAA, RSS, and UAH.

b. Observationally based technique for removing diurnal drift biases

In analyzing data for which no diurnal corrections have been applied, the implications of the diurnal drift bias become immediately clear for long-term trends. Over land, brightness temperature differences between coorbiting satellites or differences between the ascending (PM) and descending (AM) node of a single satellite can drift by more than 1 K as the satellite drifts toward earlier or later local measurement times. Figure 1 shows the LECT for each satellite over the satellite's lifetime for the descending node (the ascending node LECT is 12 h later). This figure only includes the time periods in which we used data from each satellite. Several satellites drift more than an hour during their lifetime, which means that a large diurnal signal will be aliased into their TMT measurements.

To remove the effects of diurnal drift, we develop a regression technique for estimating a TMT diurnal cycle correction based on MSU/AMSU measurements that include diurnal drift information. In section 3, we created a gridded monthly TMT time series that included warm target bias corrections but not diurnal drift corrections. These uncorrected data will allow us to estimate a diurnal cycle correction. In our analysis, most satellites drift between LECT values of 0130 and 0800 (1330 and 2000) for the descending (ascending) nodes (see Fig. 1). Over the tropical ocean, the GCM diurnal cycle is well approximated with a quadratic function during these hours for both the AM and PM nodes. Over tropical land, however, the diurnal cycle has more inflection points and is better approximated with a cubic fit (the normalized residuals for fits to the GCM diurnal cycle are reduced by a factor of ~2–3 using a cubic

rather than a quadratic function). We can then write down the measured land brightness temperature for given month as

$$T_{i,N}^M = T^E + \alpha_i T_i^W + a_{I,N} t_i^3 + b_{I,N} t_i^2 + c_{I,N} t_i + d_{i,N} + \varepsilon_i, \quad (1)$$

where T^E is the actual unbiased Earth temperature, T^M is the measured temperature, α is the warm target factor, T^W is the warm target temperature anomaly, and ε represents unresolved errors for the ith satellite. The constants a, b, and c are the coefficients for the diurnal cycle correction, and d represents a constant offset for each node of each satellite. Our diurnal cycle is dependent on the LECT t, and the coefficients vary by the MSU or AMSU instrument I and the node N. The measured ocean brightness temperature can similarly be written as

$$T_{i,N}^M = T^E + \alpha_i T_i^W + e_{I,N} t_i^2 + f_{I,N} t_i + g_{i,N} + \varepsilon_i, \quad (2)$$

where, in this case, e and f are the diurnal cycle coefficients, and g is a constant offset.

Our numerical regression technique relies on being able to attribute differences between satellites to a common diurnal cycle, which we represent via 12 coefficients for land (3 terms in the cubic fit times 2 instruments and 2 nodes) and 8 coefficients for the ocean (2 terms in the quadratic fit times 2 instruments and 2 nodes). By first removing the warm target effect in the monthly gridding process, we can ignore the warm target temperature term. Our strategy is then to fit intersatellite differences using the following equation for land based on Eq. (1):

$$\begin{aligned}
T_{i,N_1}^M - T_{j,N_2}^M &= (a_{I_1,N_1} t_i^3 + b_{I_1,N_1} t_i^2 + c_{I_1,N_1} t_i + d_{i,N_1}) \\
&\quad - (a_{I_2,N_2} t_j^3 + b_{I_2,N_2} t_j^2 + c_{I_2,N_2} t_j + d_{j,N_2}) \\
&\quad + \varepsilon_i - \varepsilon_j \quad\quad (3)
\end{aligned}$$

and the following equation for ocean from Eq. (2):

$$\begin{aligned}
T_{i,N_1}^M - T_{j,N_2}^M &= (e_{I_1,N_1} t_i^2 + f_{I_1,N_1} t_i + g_{i,N_1}) \\
&\quad - (e_{I_2,N_2} t_j^2 + f_{I_2,N_2} t_j + g_{j,N_2}) + \varepsilon_i - \varepsilon_j, \quad (4)
\end{aligned}$$

where i and j represent the satellites under consideration. The coefficients for our diurnal cycle correction vary by instrument I and node N, but it is not necessary to use the same node or instrument for satellites i and j in Eqs. (3) and (4). In other words, we do not need to compare two satellites with the same instrument or node. We have therefore denoted the instrument I and node N with subscripts 1 and 2 (for the two measurements being

compared) to make it clear that N_1 and N_2 and I_1 and I_2 are not necessarily equal to one another.

From Eqs. (3) and (4), we can use monthly brightness temperature differences from coorbiting satellites (i.e., $i \neq j$) and differences between the ascending and descending node of the same satellite (i.e., $i = j$ and $N_1 \neq N_2$) to solve for the diurnal cycle coefficients using multiple linear regression. This procedure is similar to that used for determining warm target factors for each satellite, but in this case we are fitting higher-order functions (a quadratic and cubic for ocean and land, respectively), and we use LECT as a predictor instead of the warm target temperature anomaly. We use LECT values between 0000 and 1200 for both the ascending and descending nodes, even though the ascending node is in the afternoon ($+12\,\mathrm{h}$). In our analysis we use monthly means, which is a time scale sufficient to track the gradual changes in LECT but still leaves more than 4000 predictands. The *NOAA-10* descending node constant offset is set to zero. We focus on the gradual diurnal drift by removing the long-term mean MSU/AMSU seasonal cycle from each satellite, although we note that the diurnal drift may also induce small changes in the seasonal cycle.

Some analyses have used Fourier series to solve for the diurnal cycle in infrared sounder (e.g., Lindfors et al. 2011) and microwave (e.g., Mo 2009; Kottayil et al. 2013) measurements. This approach uses overlapping satellites and fits brightness temperature measurements as a function of local time using a second-order Fourier series. It requires that measurements are absolutely calibrated, which cannot be guaranteed for MSU/AMSU measurements; the absolute uncertainty in the IMICA calibration is 0.5–1.0 K, with global mean intersatellite biases between 0.1 and 0.2 K (Zou and Wang 2013). Our method instead tracks the differences between satellite measurements over time and attributes these differences to diurnal sampling biases. Note that in our method we remove constant offsets for each node of each satellite, which means we do not require an absolute calibration of brightness temperature measurements. We also use the differences between satellites, which means that natural variability common to both satellites is removed, leaving diurnal sampling bias as the biggest component of slowly evolving intersatellite differences. Our method uses polynomial fits, since polynomials reproduce the diurnal cycles from climate models and are easily incorporated into our linear regression approach.

To assess the impact of the seasonal cycle on the diurnal drift bias removal, we merged our time series using a GCM correction with and without a seasonal cycle. The tropical land trend difference between the merged time series with and without a seasonal cycle was $0.006\,\mathrm{K}\,\mathrm{decade}^{-1}$. Over

TABLE 1. Average value of the diurnal cycle correction coefficients in Eqs. (1) and (2) over land and ocean in the tropics (20°S–20°N) for the MSU and AMSU instruments.

	Land			Ocean	
	a	*b*	*c*	*e*	*f*
MSU AM	0.0038	−0.0290	−0.0005	0.0040	−0.0494
MSU PM	0.0029	−0.0485	0.1262	−0.0015	0.0419
AMSU AM	0.0037	−0.0209	−0.0652	0.0105	−0.0895
AMSU PM	0.0038	−0.0690	0.1667	−0.0009	0.0091

tropical oceans, the difference is $0.001\,\mathrm{K}\,\mathrm{decade}^{-1}$. These small differences are expected since the seasonal cycle in the tropics is much smaller compared to higher latitudes, though a diurnal drift bias correction that accounts for the seasonal cycle should be developed in future efforts. Another important assumption we make in our formulation is that the diurnal cycle does not change over time. This is an assumption also made by RSS, NOAA, and UAH, though it is not necessarily true (e.g., Hansen et al. 1995). We expect that, although this assumption is not strictly true, diurnal cycle changes for TMT over the tropics are small compared to the diurnal drift bias we remove in our technique. Note that by using carefully calibrated L1C data, instrument calibration issues are small, and our regression is addressing diurnal drift biases. It is, however, still possible that our technique also removes residual instrument calibration biases that are correlated with the LECT. In this case, our observationally derived diurnal cycle correction may deviate from the real diurnal cycle, especially over the ocean where the diurnal cycle signal is small. But the trends based on this observationally derived correction are expected to be more accurate than those using the real diurnal cycle, because any residual instrument calibration biases related to satellite drift are further removed.

We solve Eqs. (3) and (4) for the MSU/AMSU diurnal cycle correction using tropical (20°N–20°S) mean time series for land and ocean. Table 1 presents the diurnal cycle correction coefficients from our multiple linear regression, which correspond to the constants presented in Eqs. (1) and (2). Figure 2 shows the tropical TMT diurnal cycle corrections derived from multiple linear regression using MSU/AMSU satellite observations compared to the diurnal cycles from the GCM (Mears et al. 2003) for MSU and AMSU over land and ocean. We show our diurnal cycle correction over ocean for completeness and transparency. Since the oceanic diurnal cycle should be small (e.g., Zou et al. 2009) this correction gives some indication of the degree that uncorrected biases remain in our time series after warm target calibration. For example, if we found large oceanic diurnal cycle corrections, this would indicate that
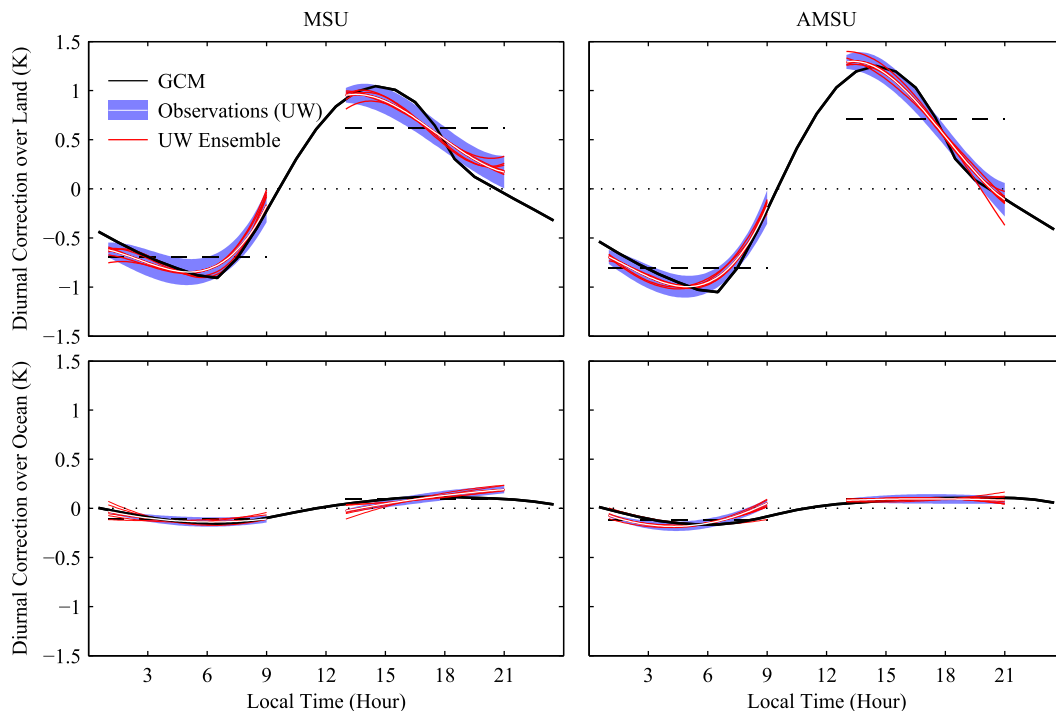
FIG. 2. Tropical mean (20°S–20°N) diurnal cycle corrections in TMT for (left) MSU and (right) AMSU over (top) land and (bottom) ocean from a GCM (black line) and from our regression analysis based on observations (white line). Blue shading represents the 95% confidence interval from our regressed diurnal cycle. We also calculated 15 diurnal cycle corrections by excluding data from each of the 15 satellites and recalculating the diurnal cycle corrections, which is represented by red lines. This ensemble shows the sensitivity to individual satellites. Since our regression removes a constant offset from each satellite node (so the absolute temperature difference between the AM and PM node is not preserved), we forced the mean of each of our regressed diurnal cycle segments (0100–0900 and 1300–2100 LT) to match the mean of the GCM over the same time period (black dashed line) to aid in comparing the GCM and regressed diurnal cycle. The GCM diurnal cycle shown here has a scaling factor of 1, though we scaled the MSU correction by 0.875 and the AMSU correction by 0.917.

calibration errors remain in the time series. From Fig. 2, we see that the ocean diurnal cycle corrections are small, indicating that large biases do not remain. For this analysis, we added white noise to our monthly average tropical mean brightness temperatures and resolved for the warm target factors and diurnal coefficients 10 000 times in order to estimate the uncertainty in our regression technique. The error estimate from this Monte Carlo analysis accounts for the uncertainty in our intersatellite offsets, warm target correction, and diurnal correction. Mears et al. (2011) do a detailed uncertainty estimate and find larger uncertainties by accounting for intersatellite trends between *NOAA-14* and *NOAA-15* and because they include diurnal uncertainty from several GCMs. We also solve for diurnal cycle corrections, which have had a single satellite of the 15 satellites removed from consideration [referred to as the University of Washington (UW) Ensemble]. The results from this sensitivity analysis show that the derived diurnal cycle correction is not very sensitive to individual

satellites (generally, the sensitivity is smaller than our estimated error in the diurnal cycle correction over land and similar in magnitude to our estimated error over ocean). Removing *NOAA-15* from the diurnal cycle calculation does reduce the magnitude of the AMSU AM ocean diurnal cycle but also increases the magnitude of the AMSU PM ocean diurnal cycle correction. This likely occurs because *NOAA-15* is an important satellite for solving for the AMSU diurnal cycle correction, since it drifts through much of the diurnal cycle. When we remove *NOAA-15*, the diurnal cycle later than 1500 LT for the ascending node and 0300 LT for the descending node is unconstrained for AMSU measurements. We also solved for the diurnal cycle correction without applying a warm target correction, and the resulting diurnal cycle corrections were negligibly different compared to those with a warm target correction (not shown). This result implies that instrument calibration drifts are not systematically aliased into our diurnal cycle.

Our derived diurnal cycle correction is similar to that produced from a climate model, but there are notable differences in the phase and amplitude over land for each node. However, we do not expect our observationally derived diurnal cycle correction would necessarily agree with one derived from a GCM. This is because our correction may include residual calibration biases that are correlated with the diurnal cycle, and the GCM diurnal cycle may also have biases. Other observational studies have noted differences in the representation of phase and amplitude in the diurnal cycle over land compared to GCMs (e.g., Dai and Trenberth 2004; Seidel et al. 2005; MacKenzie et al. 2012). For example, Dai and Trenberth (2004) show that the peak in the tropical land surface air temperature diurnal cycle occurs later in CCSM2 than in observations. We similarly find that the peak in the TMT diurnal cycle occurs earlier than in CCSM3 (Fig. 2). Note that the peaks of the tropical mean land AMSU GCM diurnal cycle used in Mears et al. (2011) occur at approximately 1230, 1330, and 1430 LT for MERRA, HadGEM, and CCSM3 (C. Mears 2014, personal communication). Our tropical mean AMSU land peak occurs at ~1320 LT, which is well within the range of model estimates. We also note that differences in the amplitude between the MSU and AMSU diurnal cycle are also enhanced in the UW-derived diurnal cycle correction compared to the GCM. We expect the AMSU diurnal amplitude to be larger over land, because the AMSU weighting function peaks closer to the surface than the MSU weighting function.

The diurnal cycle correction over the ocean is small (see Fig. 2) and the difference between tropical ocean trends with and without a diurnal cycle correction is negligible (0.002 K decade^{-1} from Table 3). Although much of our derived ocean diurnal cycle correction is significantly different from zero, the corrections, when applied to the drifting satellite data, are not statistically significant. This suggests that a significant bias is detected, but this bias has a negligible impact on our time series. The AMSU AM ocean diurnal cycle correction and the MSU PM diurnal cycle correction are larger in our technique compared to the GCM. These differences may be caused by residual calibration biases that are correlated with the diurnal cycle and/or GCM biases. Other studies (e.g., Dai and Trenberth 2004; Seidel et al. 2005; MacKenzie et al. 2012), noted that the amplitude of GCM diurnal cycles over ocean is underestimated relative to observations. Over the ocean, the observationally derived diurnal correction for MSU has increasing temperatures during the afternoon, but that for AMSU has relatively constant temperatures. It is not obvious which afternoon oceanic diurnal cycle correction is closer to the real diurnal cycle. Note that the peak

in the AMSU tropical ocean diurnal cycle is approximately 1530, 1930, and 2030 LT for HadGEM, MERRA, and CCSM3, respectively (C. Mears 2014, personal communication). The inconsistency in observationally derived MSU and AMSU oceanic diurnal cycle corrections suggests that residual calibration biases are present. Regardless, these biases are effectively removed through our diurnal cycle correction, which has a negligible effect on our derived trends. Our results indicate that our oceanic diurnal cycle correction represents a combination of a small diurnal cycle and small residual calibration corrections.

The possibility that unresolved errors introduce a significant impact on our observationally derived diurnal cycle correction is likely small, since removing individual satellites from consideration typically produces diurnal cycles within the uncertainty of our regression (Fig. 2). Some satellites, such as *NOAA-14* or *NOAA-15*, do have greater influence over our derived diurnal cycle correction and also have unexplained trend differences in their times series (e.g., Mears and Wentz 2009; Mears et al. 2011), which could be aliased into our regression technique. Since instrument calibration drift is similar for the ascending and descending node, incorporating ascending minus descending TMT comparisons into our diurnal cycle correction estimate helps minimize the effect of instrument calibration drift biases. The insensitivity of the diurnal cycle estimate to our treatment of the warm target bias also indicates that there is not a large influence of instrument calibration drift on our analysis.

We further solve for the diurnal cycle correction as a function of latitude and surface type (land or ocean) within the tropics. This approach allows us to construct the spatial evolution of TMT and to determine the combined (land and ocean) tropical TMT time series, though we note that the land and ocean trends using this gridded method are the same as those calculated using tropical mean data. In this calculation, grid cells containing greater (less) than 50% land fraction are considered as land (ocean). We solve Eqs. (3) and (4) for the diurnal cycle correction coefficients for land and ocean in each latitude band, respectively. We then apply the diurnal correction and constant offsets equally to all of the respective land or ocean grid points in that zonal band. We tested to see if the zonal spatial scale or the annual mean diurnal correction had a large influence on our results by applying a tropical, annual mean GCM land and ocean correction to each land and ocean grid cell, respectively. This test forces all regions (e.g., convective versus nonconvective) to share a common tropical mean diurnal cycle with no seasonal dependence, even though it has been demonstrated that the diurnal cycle varies between convective and nonconvective regions and over the seasonal cycle (e.g., Tian et al. 2004; Yang and
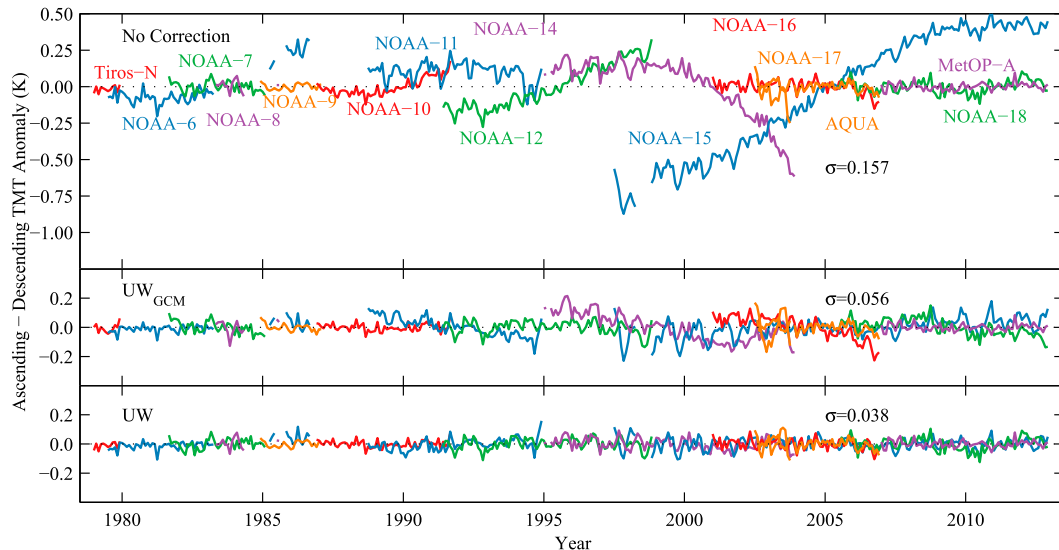
FIG. 3. Time series of the ascending minus descending node for each satellite over tropical (20°S–20°N) land using TMT (top) without diurnal corrections, (middle) with diurnal drift corrections following a diurnal cycle from a GCM, and (bottom) with corrections from our regression technique.

Slingo 2001). The tropical land trend difference versus the full GCM correction was $0.010\,\mathrm{K\,decade^{-1}}$ and less than $0.005\,\mathrm{K\,decade^{-1}}$ over ocean. These sensitivity experiments demonstrate that although the spatial pattern of the diurnal cycle evolution (e.g., across varied surface characteristics within a latitude band or over regions varied convection) may be important locally, they do not have large effects on the tropical mean TMT warming. The remainder of the analysis will be based on our gridded TMT dataset that utilizes zonal diurnal corrections. We will refer to data corrected with our observationally derived diurnal correction as UW data and data processed with a GCM diurnal correction as $\mathrm{UW_{GCM}}$.

c. The efficacy of observationally derived TMT diurnal cycle corrections

Figure 3 presents the time series of differences between the ascending and descending nodes for satellites over tropical land without a diurnal correction, with a correction using a GCM diurnal cycle ($\mathrm{UW_{GCM}}$), and with our observationally derived diurnal cycle correction (UW). Comparing differences in the AM and PM nodes of satellites is an important check for removing diurnal drifts, because instrument calibration drift should be similar in both the ascending and descending node [reducing the effect of ε in Eqs. (3) and (4)]. Removing the diurnal drift with a GCM diurnal cycle is generally effective but leaves small residual trends in the ascending minus descending difference time series. Our regression approach further reduces residuals and trends between the ascending and descending nodes.

Effectively removing diurnal drifts should also lead to near-zero differences between satellites for monthly mean brightness temperatures. Figure 4 presents the differences in tropical land anomalies between satellites for various pairs of ascending nodes for TMT data with no diurnal correction, data corrected with a GCM diurnal cycle ($\mathrm{UW_{GCM}}$), and data corrected using our observationally derived diurnal cycle correction (UW). We chose to display the ascending node because of larger drifts in this node, providing a powerful test of our technique. We attempted to choose pairs of satellites in which one satellite is relatively stable (i.e., not rapidly drifting east or west relative to the sun) while the comparison satellite has large drifts (see Fig. 1). The colors of the residuals represent the LECT of the rapidly drifting satellite, which generally cools (warms) relative to our comparison satellite as it drifts later (earlier) in the day if no diurnal corrections are applied. Figure 4 shows that, in some cases, the GCM seems to overcorrect the diurnal drift (e.g., *NOAA-11 − NOAA-12*), while in other cases, some of the diurnal signature remains (e.g., *NOAA-16 − Aqua*). The GCM diurnal bias correction is largely effective at removing intersatellite residuals and trends, but our technique further reduces these biases. Figure 1 shows that *Aqua* has almost no LECT drift because of its onboard propulsion system. In Fig. 4, the differences between *NOAA-15* and *NOAA-16* relative to *Aqua* can thus largely be attributed to the diurnal cycle. Each difference measurement demonstrated in Figs. 3 and 4 helps to constrain our fit for the diurnal cycle correction, even though there is no stable, nondrifting reference (e.g., *Aqua* or *MetOp-A*)
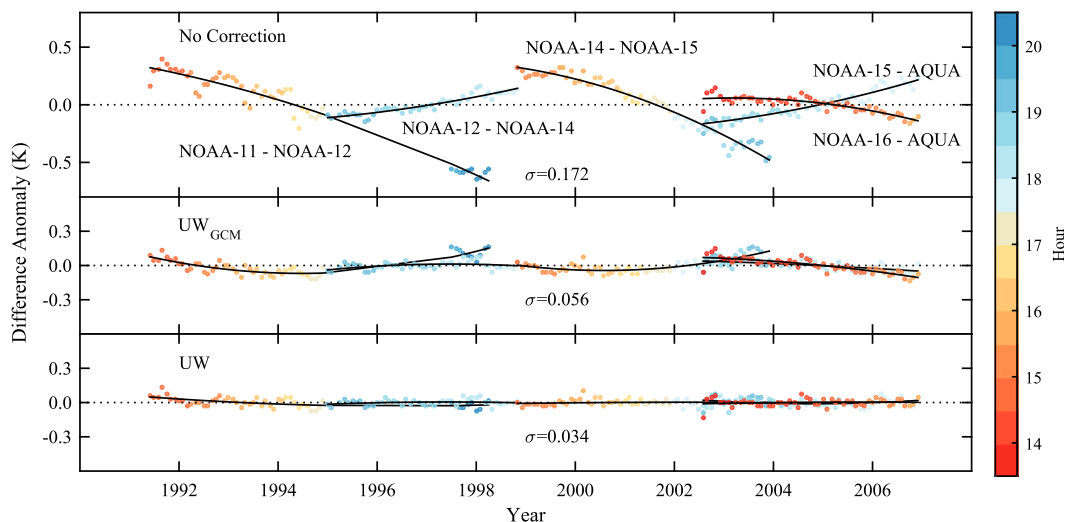
FIG. 4. Time series of differences between pairs of satellites for the ascending node over tropical (20°S–20°N) land using TMT (top) without diurnal drift corrections, (middle) with diurnal corrections following a diurnal cycle from a GCM, and (bottom) with corrections from our regression technique. We chose these pairs of satellites and the ascending node over land to maximize diurnal drift biases. For each pair (i.e., satellite 1 − satellite 2), satellite 1 is rapidly drifting, while satellite 2 has relatively little diurnal drift. The color of each point represents the LECT of the drifting satellite 1 for reference. Quadratic fits to the data are shown to aid in visualization.

for the bulk of the time series. Using all overlaps helps to ensure that unresolved or unknown instrument problems do not give us spurious results.

To characterize the overall effectiveness of our method, we show the intersatellite residual standard deviation in Table 2. Intersatellite biases over land are effectively reduced using a GCM diurnal correction (UW$_{GCM}$) and our diurnal correction (UW), as compared to the case in which no diurnal corrections are applied. Our correction represents a small but robust improvement compared to the GCM correction. Figures 3 and 4 and Table 2 illustrate that our diurnal correction appears to be successful in removing intersatellite biases due to diurnal drift.

5. TMT time series and trends and comparisons with UAH, RSS, and NOAA

We remove the diurnal drift biases, warm target effect, and constant offsets from each satellite time series and average over all of the satellites and both the ascending and descending nodes to form a homogenized MSU/AMSU TMT time series. Figure 5 presents the UW TMT time series for the tropical mean over land, ocean, and over both the land and ocean. As with other MSU/AMSU datasets, there is strong coherence between the land and ocean time series in the tropics, because the tropics do not maintain strong temperature gradients. El Niño–Southern Oscillation is an evident feature, especially the large El Niño event during 1997/98. Our TMT time series is quite similar to that from other research groups (not shown).

Figure 6 presents the probability distribution functions of our tropical TMT trends over land and ocean along with trend values from other groups. This calculation utilizes our diurnal correction performed over the tropical land and ocean with the ensemble of trend values coming from our Monte Carlo simulation described in section 4b. We find a mean tropical land trend of 0.104 ± 0.035 K decade^{-1} and a mean tropical ocean trend of 0.118 ± 0.020 K decade^{-1} (95% confidence interval). Note that this uncertainty is related to the uncertainty in our diurnal cycle and warm target corrections and does not include uncertainties related to sampling or structural uncertainties. Mears et al. (2011) undertook a comprehensive uncertainty analysis using a Monte Carlo estimation technique; the resulting RSS trend uncertainty is shown in Fig. 6. Even though the differences between groups can be large, these differences are not necessarily significant when the full internal uncertainty is considered.

TABLE 2. Average monthly intersatellite residual standard deviation (σ) for TMT without diurnal corrections (no correction), UW, and UW$_{GCM}$. We show results for the tropical (20°S–20°N) land, ocean, and land–ocean averages. The value displayed is a weighted average of the standard deviation of all coorbiting satellites with at least 6 months of overlap.

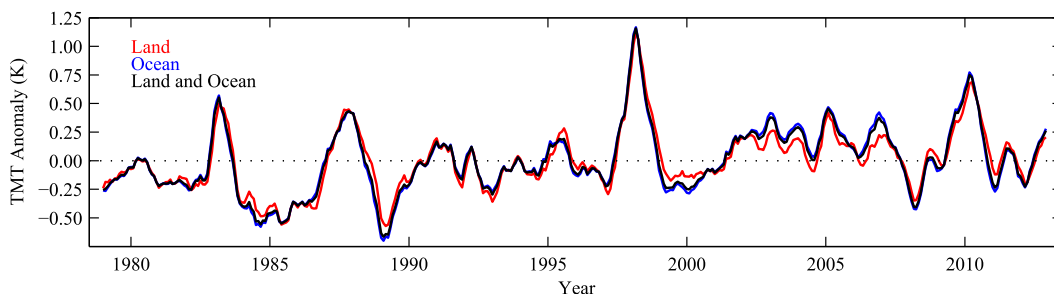|	Intersatellite residual σ (K)		
	Both	Ocean	Land
No correction	0.020	0.019	0.052
UW$_{GCM}$	0.021	0.020	0.035
UW	0.017	0.018	0.027

FIG. 5. Time series of UW TMT for the tropics (20°S–20°N) for land (red), ocean (blue), and combined land–ocean (black) over 1979–2012. The time series is smoothed using a 5-month moving average.

Figure 7 presents maps of tropical TMT trends over 1979–2012 based on our regression technique (UW), our data corrected with a GCM diurnal cycle (UW$_{GCM}$), and trends from the UAH, RSS, and NOAA datasets. UW, RSS, and NOAA have a similar warming pattern, though RSS also has a noticeably larger region of cooling in the subtropical Pacific Ocean. The most striking difference is that UAH has large negative cooling throughout most of the Pacific Ocean and has less warming in the other ocean basins. UAH and RSS also lack the cooling areas over the African and Australian continents that are present in both the UW and NOAA datasets.

Table 3 presents the tropical mean TMT trends over 1979–2012. In the table, we include uncertainty estimates for RSS (Mears et al. 2011) and for UW, which are based on the uncertainty in merging and bias removal procedures. We can also calculate the statistical uncertainty in the trend for each group. The 95% confidence

interval in the least squares linear trend estimates, accounting for autocorrelation, is roughly the same for each dataset: approximately ± 0.10 K decade^{-1} over land, ± 0.12 K decade^{-1} over ocean, and ± 0.12 K decade^{-1} for land and ocean. For the UW time series, the warm target correction reduces trends across land and ocean by 0.023 K decade^{-1}. The diurnal correction is a small positive correction over ocean (0.002 K decade^{-1}), but a very large and positive correction over land (0.160 K decade^{-1}). In general, our trends corrected with a GCM and trends corrected with our observationally derived diurnal cycle correction are similar to trends from NOAA and RSS, though RSS has less
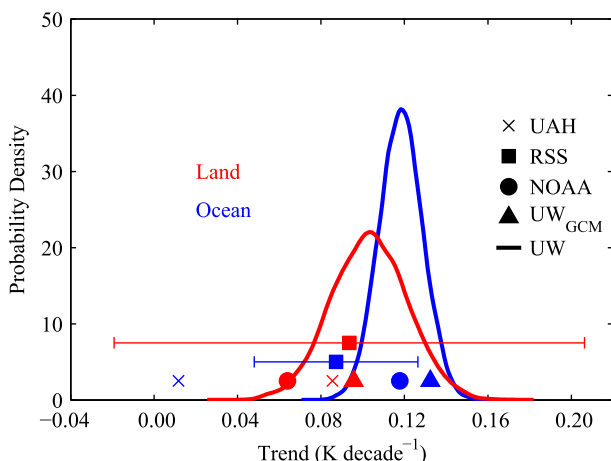

FIG. 6. Probability distribution function of tropical (20°S–20°N) UW TMT land (red) and ocean (blue) trends over 1979–2012 from this study. We also show the trends for UW$_{GCM}$, NOAA, RSS, and UAH for comparison. We include the uncertainty values for RSS trend calculation using data from Mears et al. (2011). The UW distribution represents the results when we add noise in our regression for the warm target factors and diurnal cycle correction and then remerge all of the satellites together 10 000 times.
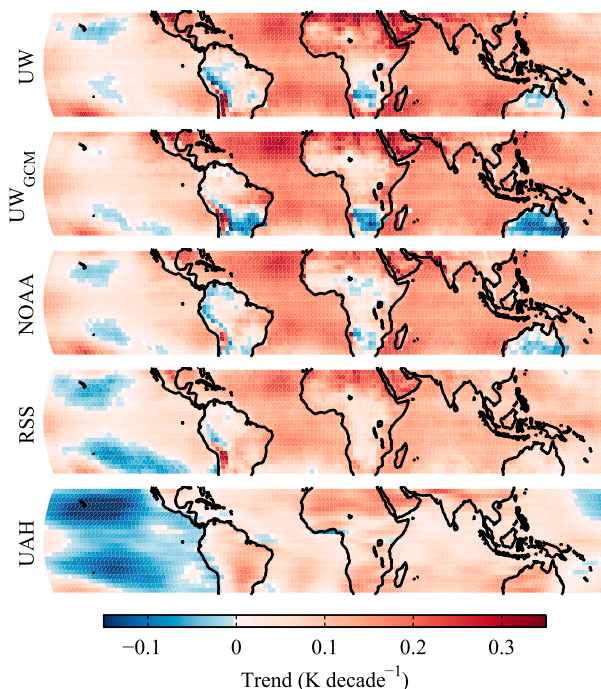
FIG. 7. Tropical (30°S–30°N) spatial pattern of TMT trends (K decade^{-1}) from various MSU/AMSU datasets over 1979–2012. We merged the MSU/AMSU observations together using both our regression technique based on observations (UW) and a GCM diurnal drift correction (UW$_{GCM}$) with other processing choices the same.

TABLE 3. Trends (K decade⁻¹) over 1979–2012 for TMT over the tropics (20°S–20°N) for TMT without diurnal corrections (no diurnal correction), UW, and UW$_{GCM}$. The trends from NOAA, RSS, and UAH are listed for reference. The 95% confidence intervals on UW trends are from our Monte Carlo simulation. The 95% confidence interval for RSS are based on data updated since Mears et al. (2011).

	TMT trend (K decade⁻¹)		
	Both	Ocean	Land
No diurnal correction	0.075	0.116	−0.056
UW	0.115 ± 0.024	0.118 ± 0.020	0.104 ± 0.035
UW$_{GCM}$	0.124	0.132	0.096
NOAA	0.105	0.118	0.064
RSS	0.089 ± 0.051	0.087 ± 0.039	0.094 ± 0.113
UAH	0.029	0.012	0.085

warming over ocean and NOAA has less warming over land. As demonstrated in Table 3 and Figs. 6 and 7, the UAH ocean trend is notably lower than trends from all other datasets. Differences among various TMT datasets over the tropics will be interpreted in detail in section 6.

One drawback of TMT trends is that they include some influence from the stratosphere, which has a large negative temperature trend. It has been demonstrated that this influence can be removed using TLS from MSU channel 4 and AMSU channel 9 to provide a measure of the full tropospheric temperature (T24) trend (e.g., Fu et al. 2004; Fu and Johanson 2004, 2005). In Table 4, we provide tropical T24 trends, surface temperature trends from HadCRUT4, and the amplification ratio of the T24 trend to the surface trend. Our amplification factor over the tropics is consistent with tropical tropospheric amplification implied by models, which is approximately

TABLE 4. T24 trends (K decade⁻¹) over 1979–2012 in the tropics (20°S–20°N) over land, ocean, and the entire tropical region, as derived from various MSU/AMSU datasets. The values in parentheses are the amplification ratio, which is defined here as the T24 trend divided by the HadCRUT4 surface trend. We compute T24 using T24 = 1.1TMT − 0.1TLS. The UW and UW$_{GCM}$ T24 trends are calculated using TMT from the present study and TLS from NOAA STAR v3.0 data.

Group	Both	Ocean	Land
UW	0.160 (1.41)	0.163 (1.62)	0.150 (0.86)
UW$_{GCM}$	0.170 (1.50)	0.179 (1.78)	0.141 (0.81)
NOAA	0.149 (1.32)	0.163 (1.62)	0.106 (0.61)
RSS	0.125 (1.10)	0.123 (1.22)	0.133 (0.76)
UAH	0.064 (0.56)	0.044 (0.44)	0.129 (0.73)
HadCRUT4	0.114	0.101	0.175

1.4–1.6 (Santer et al. 2005; Fu et al. 2011). Our amplification factor over land is reduced because of enhanced land surface warming relative to sea surface warming (e.g., Sutton et al. 2007). All of the MSU/AMSU datasets demonstrate tropical tropospheric amplification, except UAH.

6. Interpreting TMT time series differences between MSU/AMSU datasets

Figure 8 shows TMT from each group minus the UW TMT time series over the tropics. It contains several notable features. Relative to the UW dataset over land, RSS, NOAA, and UW$_{GCM}$ slowly cool from 1979 to 1995. RSS, NOAA, and UW$_{GCM}$ also show warming after 2000 over land, followed by cooling after 2003 relative to UW TMT. Over ocean, RSS cools relative to UW near 1985–87 and near 2004. NOAA warms relative to UW near 1998 and cools after 2003. We note that 1985–87 differences are likely a result of the *NOAA-9* target factor
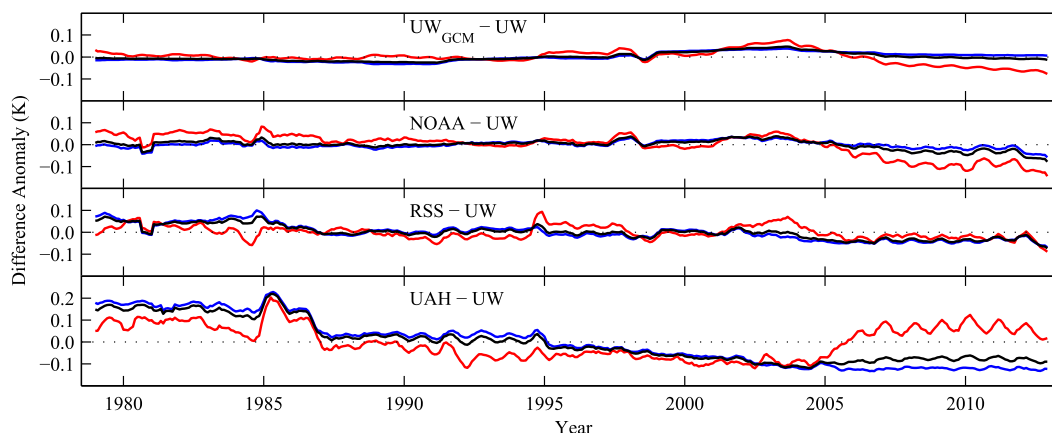

FIG. 8. Tropical (20°S–20°N) land (red), ocean (blue), and combined land–ocean (black) difference time series for NOAA, RSS, and UAH minus UW. A time series of UW$_{GCM}$ is also shown to understand the differences caused by diurnal cycle corrections (all other processing decisions are held constant between UW and UW$_{GCM}$). The time series are smoothed using a 5-month moving average.
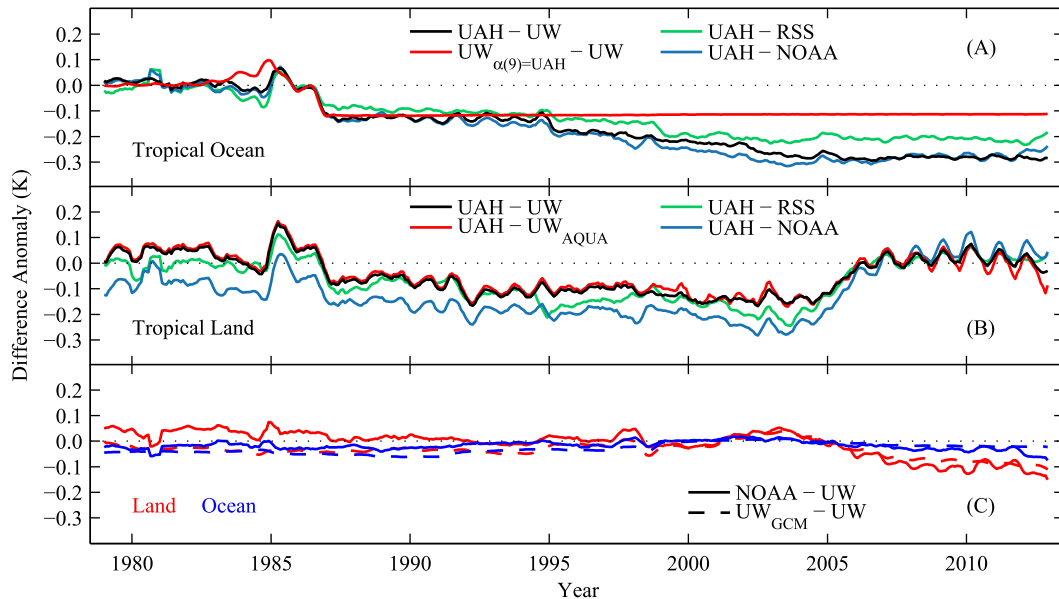
FIG. 9. (a) Tropical (20°S–20°N) ocean TMT time series for UAH minus UW, RSS, and NOAA. Ocean TMT data are used to minimize the influence of the diurnal cycle. UW data are also compared to data in which we force the *NOAA-9* target factor to match the UAH value of 0.0986 [UW$_{\alpha(9)=UAH}$]. Each time series is smoothed using a 5-month moving average and has anomalies computed relative to the 1985–87 time period for comparison purposes. (b) Tropical (20°S–20°N) land time series for UAH TMT minus UW, RSS, and NOAA TMT. The land time series is used here to understand the diurnal cycle bias corrections after 2005. Smoothed time series anomalies are displayed relative to the 2005–11 time period for comparison purposes. We also use UW TMT time series in which we remove *NOAA-15*, *NOAA-16*, *NOAA-17*, and *NOAA-18* from our time series (UW$_{AQUA}$), which forces our data to rely on the *Aqua* satellite in the mid-2000s (since *Aqua* has no diurnal drift, UW$_{AQUA}$ cannot have a diurnal drift bias). (c) Comparison of NOAA TMT − UW TMT for tropical (20°S–20°N) land (red solid line) and ocean (blue solid line). We also display UW$_{GCM}$ − UW for land (red dashed line) and ocean (blue dashed line) to understand the differences causes by diurnal drift bias corrections. Smoothed time series anomalies are displayed relative to the 2000–07 time period.

(Po-Chedley and Fu 2012a); RSS uses a slightly larger target factor than NOAA and UW. Overall, NOAA behaves similarly to UW$_{GCM}$ over ocean and has similar features over land, especially after 1997. UAH shows a large discontinuity during 1985–87 in both land and ocean, a cooling near 1992 (1995) over land (ocean), a gradual cooling from about 1997 to 2003 over both ocean and land, and a large warming trend over land near 2005 relative to UW.

Despite the differences in both phases and magnitudes of the diurnal cycles between GCM and observations (Fig. 2), the differences in derived TMT time series between UW$_{GCM}$ and UW (Fig. 8) are small. The trend differences are less than 0.02 K decade^{-1} (Tables 3 and 4). It is indicated that the diurnal cycle from a GCM can be used to effectively remove the satellite drift biases in TMT.

In Fig. 9, we present results that aid in further understanding some of the underlying causes for difference between the tropical TMT time series. Figure 9a shows UAH minus UW, RSS, and NOAA for the tropical ocean. We utilize the tropical ocean in this case, because this reduces the effect of diurnal drift. In each of these

cases, UAH has a large discontinuity during 1985–87. In Fig. 9a we also use a time series in which we force the *NOAA-9* target factor to be the same as the UAH value, $\alpha_9 = 0.0986$ (Po-Chedley and Fu 2012a), and then re-solve for the rest of our target factors [UW$_{\alpha(9)=UAH}$] to see if we reproduce the UAH discontinuity. Our original target factor for *NOAA-9* using data in which instrument nonlinearity biases are removed via IMICA is 0.0157. The small magnitude of our target factor demonstrates that the NOAA IMICA calibration is effective at removing instrument biases. By solving for the diurnal cycle correction with these perturbed target factors, we reproduce the UAH discontinuity during 1985–87 (see the red line in Fig. 9a). Relative to UW, UW$_{\alpha(9)=UAH}$ reduces the tropical ocean TMT trend by 0.039 K decade^{-1}, which explains about one-third of the trend difference between UAH and UW over the tropical ocean (Table 3). Importantly, UAH has a similar discontinuity relative to RSS, NOAA, and UW, and the NOAA and UW effectively rely on the independent IMICA instrument calibration. Figure 9a indicates that UAH has a problem with its bias removal during the 1985–87 period. Our recent work

showed that the UAH *NOAA-9* target factor has a positive bias of ~0.05–0.08 based on radiosondes and in comparisons between UAH *NOAA-9* and *NOAA-6* data (Po-Chedley and Fu 2012a, 2013; Christy and Spencer 2013). This bias leads to a contamination of *NOAA-9* warm target temperatures in the UAH TMT dataset, causing a global artificial cooling trend of about 0.035 K decade^{-1} over 1979–2009 (Po-Chedley and Fu 2013). UAH uses land and ocean data to solve for its target factors. One potential approach to understand this bias is to use UAH global ocean data with and without a diurnal cycle bias correction to solve for the warm target factors. Since the target factors are meant to minimize errors in instrument calibration, the target factors should be invariant for land and ocean. If the target factors change using UAH oceanic data, it would suggest that a UAH diurnal cycle bias correction is influencing the warm target calibration. The ocean diurnal correction should also have a small effect on the target factors, since the diurnal cycle over the ocean is small. UAH also utilizes seasonal smoothing and a subset of satellites to determine its *NOAA-9* target factor, which may also contribute to this difference (Po-Chedley and Fu 2013). The UAH data, as is, suggest that the warming of the tropical troposphere is decoupled from the tropical oceanic warming. On the other hand, three independent MSU/AMSU analyses find a much lower target factor value for *NOAA-9*, which is also supported by analysis based on independent observations (Po-Chedley and Fu 2012a, 2013).

The UAH tropical TMT land trend is closer to that of RSS, NOAA, and UW largely because of strong warming after 2004. Christy et al. (2010) suggested that, after 2001, model-based diurnal corrections for TLT results in artificial warming for *NOAA-14* and even greater artificial cooling for *NOAA-15*, which lead to greater consistency between UAH and RSS by 2008. Figure 9b shows the UAH tropical land time series relative to UW, RSS, and NOAA. In this case, we utilize the tropical land time series to emphasize differences related to the diurnal drift correction. UAH has strong warming near 2005 relative to all of the comparison datasets. Note that UW applied an observationally based diurnal drift correction while RSS and NOAA used a GCM-derived correction. To further test whether this difference is caused by diurnal drift corrections used in UW, RSS, and NOAA, we remove *NOAA-15*, *NOAA-16*, *NOAA-17*, and *NOAA-18* to form a new time series (UW$_{AQUA}$), which means that TMT from brightness temperatures largely rely on *Aqua* from 2002–06 and *MetOp-A* afterward. Since *Aqua* and *MetOp-A* do not have diurnal drift, there should be no signature of diurnal drift in UW$_{AQUA}$. Figure 9b shows that UAH − UW$_{AQUA}$ is very similar to UAH − UW and UAH still has similar

strong land warming after 2004 relative to UW$_{AQUA}$. This suggests that the UAH TMT dataset has spurious warming related to its diurnal drift correction. In TMT v5.6, UAH uses satellites that have relatively little diurnal drift and does not apply corrections for satellites carrying AMSU, which may leave spurious warming during *NOAA-15*'s lifetime (J. Christy 2013, personal communication). Comparisons between *NOAA-15* and *NOAA-16* with *Aqua* may help resolve this issue.

Figures 8 and 9a suggest that much of the UAH tropical trend difference relative to other datasets is due to the *NOAA-9* target factor, with more gradual changes during 1995–2005, which also contribute to the discrepancy. A spurious UAH tropical land trend after 2005 relative to other TMT datasets and our analysis with drifting satellites removed suggest that the UAH treatment of diurnal drift has biases. Unlike the RSS and NOAA diurnal corrections, the UAH correction is not publicly available for comparison. UAH constructs its TMT diurnal drift correction using 13 months of data from three coorbiting AMSU satellites: *NOAA-15*, *NOAA-16*, and *NOAA-17* (J. Christy 2013, personal communication). Differences between our approach and UAH likely result because UAH does not apply diurnal corrections to AMSU measurements (AMSU was carried on satellites starting with *NOAA-15*). It is also possible that diurnal corrections calculated with AMSU may have biases when applied to MSU. A further complication is that the three coorbiting satellites need to be absolutely calibrated, which is not possible with AMSU, since MSU/AMSU radiometers are not International System of Units (SI) calibrated. Furthermore, the correction derived from six unique points may be sensitive to assumptions regarding the shape of the diurnal cycle.

Figure 9c shows NOAA − UW for both tropical land and ocean. We also plot UW$_{GCM}$ − UW, which isolates the differences due to the GCM diurnal correction versus our observationally based approach, since other processing steps are the same. This UW − UW$_{GCM}$ comparison shows that slightly enhanced warming over the tropical ocean may be a result of the GCM-derived diurnal drift correction, though the trend difference is very small (0.014 K decade^{-1}). The upward and then downward trends in NOAA and RSS tropical land between 2000 and 2007 (Figs. 8 and 9c), similar to those in UW$_{GCM}$, are caused by the difference between the GCM- and observationally based diurnal corrections. This behavior may be due to the residual trends in *NOAA-14*, *NOAA-15*, and *NOAA-16* (Figs. 3 and 4), which was also noted in Christy et al. (2010) for TLT. Since our diurnal drift correction is observationally based and also improves error characteristics in the tropical TMT time series relative to a GCM, these features in the NOAA (and

RSS) time series may be artificial, owing to the use of the GCM-simulated diurnal cycle. This statement is further enforced by examining the difference between NOAA and UW_{AQUA} (not shown). It is also noted that the small jump in 1997/98 in NOAA − UW appears to be related to the reemergence of *NOAA-11* in the time series (see Figs. 4 and 8). UW warms relative to NOAA over land prior to 1998. We utilize different time periods for the satellites compared to NOAA and find that there is some sensitivity of the MSU/AMSU merged trend to the exact satellite data used. Other causes for this difference may include processing differences, such as small differences in the application of our GCM diurnal correction or warm target correction.

7. Discussion and conclusions

This study demonstrates the success of an observationally based approach to removing diurnal drift biases from the MSU/AMSU TMT record. The approach utilizes information from intersatellite differences and differences between ascending and descending nodes of individual satellites. As satellites drift through the diurnal cycle, we can compare observations at various LECTs and construct a common diurnal cycle correction for MSU and AMSU that explains differences in the TMT measurement for each satellite and node. This approach, compared to a diurnal drift bias correction derived from a climate model, has improved error characteristics, though tropical trend values utilizing the observationally based diurnal correction are very similar to trend values utilizing a GCM correction, with differences smaller than $0.02 \, \mathrm{K \, decade^{-1}}$. By deriving zonally averaged diurnal corrections over land and ocean, our approach may introduce some biases in the spatial pattern of trends over land because of different land surface characteristics in a given latitudinal band. The spatial pattern of our TMT trends, however, compares well with independent TMT datasets.

In this work, we combined TMT data with TLS to derive the T24 full tropospheric temperature, which effectively removes the influence of the stratosphere from TMT. The ratio of tropical full tropospheric T24 trends to the HadCRUT4 surface temperature trends over ocean is 0.4, 1.2, 1.6, and 1.6 from UAH, RSS, NOAA, and UW, respectively. The ratios from RSS, NOAA, and UW demonstrate tropical tropospheric amplification and are in general agreement with amplification from climate models, indicating that there is no significant discrepancy between observations and models for lapse rate changes between the surface and the full troposphere.

This work represents an independent analysis of the MSU/AMSU TMT evolution. We start the analysis using the newly released NOAA STAR L1C data that include the state-of-the-art corrections for instrument calibration biases. Our subsequent analysis using an observationally based diurnal drift correction shows that our results are generally consistent with RSS and NOAA in the tropics, even though small discrepancies exist. The focus of this work is on the tropics, given the historic debates regarding tropical tropospheric warming. Large differences between UAH and comparison datasets in the tropics are largely a result of differences in the *NOAA-9* target factor and differences in diurnal drift corrections. Although this is generally referred to as a structural uncertainty, careful comparisons between coorbiting satellites and between the ascending and descending node on individual satellites may help resolve these discrepancies. Work by Po-Chedley and Fu (2012a, 2013), through multiple lines of evidence, suggests that the UAH *NOAA-9* target factor is too large. This bias explains roughly one-third of the trend difference in the tropical ocean between UAH and UW. Evidence of diurnal drift bias in the UAH TMT dataset after 2005 was presented in this work. Christy et al. (2011) has suggested the large differences between UAH and RSS (NOAA) in the tropical TMT time series are due to RSS diurnal drift biases that are prominent around 1992, though Mears et al. (2012) demonstrate that evidence presented for these claims is dependent on the datasets and the methodology and ignores the large uncertainty in observations. Our independent analysis based on an observationally derived diurnal cycle correction also shows differences between UAH and UW in the 1990s, especially a gradual cooling relative to UW during 1995–2005. These differences could be due to a number of effects, including data treatment, warm target calibration, and diurnal drift. In the future, it would be useful if each dataset provider made individual satellite node time series and bias corrections available for intercomparison, since this work shows that these comparisons can be helpful in advancing understanding of biases in the MSU/AMSU TMT dataset.

REFERENCES

Christy, J. R., and W. B. Norris, 2006: Satellite and VIZ–radiosonde intercomparisons for diagnosis of nonclimatic influences. *J. Atmos. Oceanic Technol.,* **23,** 1181–1194, doi:10.1175/JTECH1937.1.

——, and R. W. Spencer, 2013: Comments on "A bias in the midtropospheric channel warm target factor on the *NOAA-9* Microwave Sounding Unit." *J. Atmos. Oceanic Technol.,* **30,** 1006–1013, doi:10.1175/JTECH-D-12-00107.1.

——, ——, and E. S. Lobl, 1998: Analysis of the merging procedure for the MSU daily temperature time series. *J. Climate,* **11,** 2016–2041, doi:10.1175/1520-0442-11.8.2016.

——, ——, and W. D. Braswell, 2000: MSU tropospheric temperatures: Dataset construction and radiosonde comparisons. *J. Atmos. Oceanic Technol.,* **17,** 1153–1170, doi:10.1175/1520-0426(2000)017<1153:MTTDCA>2.0.CO;2.

——, ——, W. B. Norris, W. D. Braswell, and D. E. Parker, 2003: Error estimates of version 5.0 of MSU–AMSU bulk atmospheric temperatures. *J. Atmos. Oceanic Technol.,* **20,** 613–629, doi:10.1175/1520-0426(2003)20<613:EEOVOM>2.0.CO;2.

——, W. B. Norris, R. W. Spencer, and J. J. Hnilo, 2007: Tropospheric temperature change since 1979 from tropical radiosonde and satellite measurements. *J. Geophys. Res.,* **112,** D06102, doi:10.1029/2005JD006881.

——, and Coauthors, 2010: What do observational datasets say about modeled tropospheric temperature trends since 1979? *Remote Sens.,* **2,** 2148–2169, doi:10.3390/rs2092148.

——, R. W. Spencer, and W. B. Norris, 2011: The role of remote sensing in monitoring global bulk tropospheric temperatures. *Int. J. Remote Sens.,* **32,** 671–685, doi:10.1080/01431161.2010.517803.

Dai, A., and K. E. Trenberth, 2004: The diurnal cycle and its depiction in the Community Climate System Model. *J. Climate,* **17,** 930–951, doi:10.1175/1520-0442(2004)017<0930:TDCAID>2.0.CO;2.

Douglass, D. H., J. R. Christy, B. D. Pearson, and S. F. Singer, 2008: A comparison of tropical temperature trends with model predictions. *Int. J. Climatol.,* **28,** 1693–1701, doi:10.1002/joc.1651.

Fu, Q., and C. M. Johanson, 2004: Stratospheric influences on MSU-derived tropospheric temperature trends: A direct error analysis. *J. Climate,* **17,** 4636–4640, doi:10.1175/JCLI-3267.1.

——, and ——, 2005: Satellite-derived vertical dependence of tropical tropospheric temperature trends. *Geophys. Res. Lett.,* **32,** doi:10.1029/2004GL022266.

——, ——, S. G. Warren, and D. J. Seidel, 2004: Contribution of stratospheric cooling to satellite-inferred tropospheric temperature trends. *Nature,* **429,** 55–58, doi:10.1038/nature02524.

——, S. Manabe, and C. M. Johanson, 2011: On the warming in the tropical upper troposphere: Models versus observations. *Geophys. Res. Lett.,* **38,** L15704, doi:10.1029/2011GL048101.

Goldberg, M. D., D. S. Crosby, and L. Zhou, 2001: The limb adjustment of AMSU-A observations: Methodology and validation. *J. Appl. Meteor.,* **40,** 70–83, doi:10.1175/1520-0450(2001)040<0070:TLAOAA>2.0.CO;2.

Hansen, J., M. Sato, and R. Ruedy, 1995: Long-term changes of the diurnal temperature cycle: Implications about mechanisms of global climate change. *Atmos. Res.,* **37,** 175–209, doi:10.1016/0169-8095(94)00077-Q.

Jackson, D. L., and B. J. Soden, 2007: Detection and correction of diurnal sampling bias in HIRS/2 brightness temperatures. *J. Atmos. Oceanic Technol.,* **24,** 1425–1438, doi:10.1175/JTECH2062.1.

Karl, T. R., S. J. Hassol, C. D. Miller, and W. L. Murray, Eds., 2006: Temperature trends in the lower atmosphere: Steps for understanding and reconciling differences. Climate Change Science Program and the Subcommittee on Global Change Research Rep., 164 pp. [Available online at http://data.globalchange.gov/assets/51/56/6d7da49e1f93bef673d56ff6aa6a/sap1-1-final-all.pdf.]

Kiehl, J. T., J. J. Hack, G. B. Bonan, B. A. Boville, B. P. Briegleb, D. L. Williamson, and P. J. Rasch, 1996: Description of the NCAR Community Climate Model (CCM3). NCAR Tech. Note NCAR/TN-4201+STR, 152 pp., doi:10.5065/D6FF3Q99.

Kottayil, A., V. O. John, and S. A. Buehler, 2013: Correcting diurnal cycle aliasing in satellite microwave humidity measurements. *J. Geophys. Res.,* **118,** 101–113, doi:10.1029/2012JD018545.

Lindfors, A. V., I. A. MacKenzie, S. F. B. Tett, and L. Shi, 2011: Climatological diurnal cycles in clear-sky brightness temperatures from the High-Resolution Infrared Radiation Sounder (HIRS). *J. Atmos. Oceanic Technol.,* **28,** 1199–1205, doi:10.1175/JTECH-D-11-00093.1.

MacKenzie, I. A., S. F. B. Tett, and A. V. Lindfors, 2012: Climate model–simulated diurnal cycles in HIRS clear-sky brightness temperatures. *J. Climate,* **25,** 5845–5863, doi:10.1175/JCLI-D-11-00552.1.

Mears, C. A., and F. J. Wentz, 2005: The effect of diurnal correction on satellite-derived lower tropospheric temperature. *Science,* **309,** 1548–1551, doi:10.1126/science.1114772.

——, and ——, 2009: Construction of the Remote Sensing Systems v3.2 atmospheric temperature records from the MSU and AMSU microwave sounders. *J. Atmos. Oceanic Technol.,* **26,** 1040–1056, doi:10.1175/2008JTECHA1176.1.

——, M. C. Schabel, and F. J. Wentz, 2003: A reanalysis of the MSU channel 2 tropospheric temperature record. *J. Climate,* **16,** 3650–3664, doi:10.1175/1520-0442(2003)016<3650:AROTMC>2.0.CO;2.

——, F. J. Wentz, P. Thorne, and D. Bernie, 2011: Assessing uncertainty in estimates of atmospheric temperature changes from MSU and AMSU using a Monte-Carlo estimation technique. *J. Geophys. Res.,* **116,** D08112, doi:10.1029/2010JD014954.

——, ——, and P. W. Thorne, 2012: Assessing the value of Microwave Sounding Unit-radiosonde comparisons in ascertaining errors in climate data records of tropospheric temperatures. *J. Geophys. Res.,* **117,** D19103, doi:10.1029/2012jd017710.

Mo, T., 2009: A study of the *NOAA-15* AMSU-A brightness temperatures from 1998 through 2007. *J. Geophys. Res.,* **114,** D11110, doi:10.1029/2008JD011267.

Morice, C. P., J. J. Kennedy, N. A. Rayner, and P. D. Jones, 2012: Quantifying uncertainties in global and regional temperature change using an ensemble of observational estimates: The HadCRUT4 data set. *J. Geophys. Res.,* **117,** D08101, doi:10.1029/2011JD017187.

Po-Chedley, S., 2012: Reconciling tropospheric temperature trends from the Microwave Sounding Unit. M.S. thesis, Dept. of Atmospheric Sciences, University of Washington, 82 pp.

——, and Q. Fu, 2012a: A bias in the midtropospheric channel warm target factor on the *NOAA-9* Microwave Sounding Unit. *J. Atmos. Oceanic Technol.,* **29,** 646–652, doi:10.1175/JTECH-D-11-00147.1.

——, and ——, 2012b: Discrepancies in tropical upper tropospheric warming between atmospheric circulation models and satellites. *Environ. Res. Lett.,* **7,** 044018, doi:10.1088/1748-9326/7/4/044018.

——, and ——, 2013: Reply to "Comments on 'A bias in the midtropospheric channel warm target factor on the *NOAA-9* Microwave Sounding Unit.'" *J. Atmos. Oceanic Technol.,* **30,** 1014–1020, doi:10.1175/JTECH-D-12-00131.1.

Randall, R. M., and B. M. Herman, 2008: Using limited time period trends as a means to determine attribution of discrepancies in Microwave Sounding Unit–derived tropospheric temperature time series. *J. Geophys. Res.,* **113,** D05105, doi:10.1029/2007JD008864.

Randel, W. J., and F. Wu, 2006: Biases in stratospheric and tro-
pospheric temperature trends derived from historical radio-
sonde data. *J. Climate,* **19,** 2094–2104, doi:10.1175/JCLI3717.1.

Santer, B. D., and Coauthors, 2005: Amplification of surface tem-
perature trends and variability in the tropical atmosphere.
Science, **309,** 1551–1556, doi:10.1126/science.1114867.

——, and Coauthors, 2008: Consistency of modelled and observed
temperature trends in the tropical troposphere. *Int. J. Clima-
tol.,* **28,** 1703–1722, doi:10.1002/joc.1756.

Seidel, D. J., M. Free, and J. Wang, 2005: Diurnal cycle of upper-air
temperature estimated from radiosondes. *J. Geophys. Res.,*
110, D09102, doi:10.1029/2004JD005526.

Sherwood, S. C., J. R. Lanzante, and C. L. Meyer, 2005: Radio-
sonde daytime biases and late-20th century warming. *Science,*
309, 1556–1559, doi:10.1126/science.1115640.

——, C. L. Meyer, R. J. Allen, and H. A. Titchner, 2008: Robust
tropospheric warming revealed by iteratively homogenized
radiosonde data. *J. Climate,* **21,** 5336–5352, doi:10.1175/
2008JCLI2320.1.

Solomon, S., D. Qin, M. Manning, Z. Chen, M. Marquis, K. Averyt,
M. Tignor, and H. L. Miller Jr., Eds., 2007: *Climate Change
2007: The Physical Science Basis*. Cambridge University Press,
996 pp.

Sutton, R. T., B. Dong, and J. M. Gregory, 2007: Land/sea warming
ratio in response to climate change: IPCC AR4 model results
and comparison with observations. *Geophys. Res. Lett.,* **34,**
L02701, doi:10.1029/2006GL028164.

Thorne, P. W., and Coauthors, 2007: Tropical vertical temperature
trends: A real discrepancy? *Geophys. Res. Lett.,* **34,** L16702,
doi:10.1029/2007GL029875.

Tian, B., B. J. Soden, and X. Wu, 2004: Diurnal cycle of convection,
clouds, and water vapor in the tropical upper troposphere:
Satellites versus a general circulation model. *J. Geophys. Res.,*
109, D10101, doi:10.1029/2003JD004117.

Titchner, H. A., P. W. Thorne, M. P. McCarthy, S. F. B. Tett,
L. Haimberger, and D. E. Parker, 2009: Critically reassessing
tropospheric temperature trends from radiosondes using realistic
validation experiments. *J. Climate,* **22,** 465–485, doi:10.1175/
2008JCLI2419.1.

Wallace, J. M., and Coauthors, 2000: *Reconciling Observations of
Global Temperature Change.* National Academy Press, 86 pp.

Wang, W., and C.-Z. Zou, 2014: AMSU-A-only atmospheric
temperature data records from the lower troposphere to the
top of the stratosphere. *J. Atmos. Oceanic Technol.,* **31,** 808–
825, doi:10.1175/JTECH-D-13-00134.1.

Wentz, F. J., and T. Meissner, 1999: AMSR ocean algorithm, ver-
sion 2. Remote Sensing Systems Tech. Rep. 121599A-1, 58 pp.
[Available online at http://eospso.gsfc.nasa.gov/sites/default/
files/atbd/atbd-amsr-ocean.pdf.]

Yang, G.-Y., and J. M. Slingo, 2001: The diurnal cycle in the tropics. *Mon.
Wea. Rev.,* **129,** 784–801, doi:10.1175/1520-0493(2001)129<0784:
TDCITT>2.0.CO;2.

Zou, C.-Z., and W. Wang, 2009: Diurnal drift correction in the
NESDIS/STAR MSU/AMSU atmospheric temperature cli-
mate data record. *Atmospheric and Environmental Remote
Sensing Data Processing and Utilization V: Readiness for
GEOSS III,* M. D. Goldberg and H. J. Bloom, Eds., In-
ternational Society for Optical Engineering (SPIE Proceedings,
Vol. 7456), 74560G, doi:10.1117/12.824459.

——, and ——, 2010: Stability of the MSU-derived atmospheric
temperature trend. *J. Atmos. Oceanic Technol.,* **27,** 1960–1971,
doi:10.1175/2009JTECHA1333.1.

——, and ——, 2011: Intersatellite calibration of AMSU-A ob-
servations for weather and climate applications. *J. Geophys.
Res.,* **116,** D23113, doi:10.1029/2011JD016205.

——, and ——, 2013: MSU/AMSU radiance fundamental climate
data record calibrated using simultaneous nadir overpasses.
Climate Data Record Program Tech. Rep. CDRP-0015, 56 pp.
[Available online at http://www.star.nesdis.noaa.gov/smcd/
emb/mscat/documents/MSU_AMSU_CATBD_V1.0.pdf.]

——, M. D. Goldberg, Z. Cheng, N. C. Grody, J. T. Sullivan, C. Cao,
and D. Tarpley, 2006: Recalibration of Microwave Sounding
Unit for climate studies using simultaneous nadir overpasses.
J. Geophys. Res., **111,** D19114, doi:10.1029/2005JD006798.

——, M. Gao, and M. D. Goldberg, 2009: Error structure and at-
mospheric temperature trends in observations from the Mi-
crowave Sounding Unit. *J. Climate,* **22,** 1661–1681, doi:10.1175/
2008JCLI2233.1.